Biogenic carbon and anthropogenic pollutants combine to form a cooling haze over the southeastern United States

Allen H. Goldstein[1], Charles D. Koven[2], Colette L. Heald[3], and Inez Y. Fung[1]

Department of Environmental Science, Policy, and Management, University of California, Berkeley, CA 94720

Contributed by Inez Y. Fung, April 15, 2009 (sent for review July 28, 2008)

Remote sensing data over North America document the ubiquity of secondary aerosols resulting from a combination of primary biogenic and anthropogenic emissions. The spatial and temporal distribution of aerosol optical thickness (AOT) over the southeastern United States cannot be explained by anthropogenic aerosols alone, but is consistent with the spatial distribution, seasonal distribution, and temperature dependence of natural biogenic volatile organic compound (BVOC) emissions. These patterns, together with observations of organic aerosol in this region being dominated by modern ^{14}C and BVOC oxidation products with summer maxima, indicate nonfossil fuel origins and strongly suggest that the dominant summer AOT signal is caused by secondary aerosol formed from BVOC oxidation. A link between anthropogenic and biogenic emissions forming secondary aerosols that dominate the regional AOT is supported by reports of chemicals in aerosols formed by BVOC oxidation in a NO_x- and sulfate-rich environment. Even though ground-based measurements from the IMPROVE network suggest higher sulfate than organic concentrations near the surface in this region, we infer that much of the secondary organic aerosol in the Southeast must occur above the surface layer, consistent with reported observations of the organic fraction of the total aerosol increasing with height and models of the expected vertical distribution of secondary organic aerosols from isoprene oxidation. The observed AOT is large enough in summer to provide regional cooling; thus we conclude that this secondary aerosol source is climatically relevant with significant potential for a regional negative climate feedback as BVOC emissions increase with temperature.

aerosol | biogenic volatile organic compound | climate | remote sensing | secondary organic aerosols

The importance of biogenic volatile organic compounds (BVOC) reacting with anthropogenic oxides of nitrogen (NO_x) to cause high regional ozone concentrations during summer in the southeastern United States (SE U.S.) was first explained by Chameides et al. (1). This work fundamentally changed the understanding of regulatory approaches for controlling ozone pollution by focusing attention on the need to reduce NO_x emissions. We present evidence that similar interactions control secondary aerosol in this region in summer, when concentrations are highest, suggesting that appropriate control strategies focused on the key anthropogenic factors will be required if effects on climate and visibility are to be reduced.

The largest uncertainties in projections of radiative forcing involve the direct effects of aerosols on the Earth's radiation budget and the indirect effects through its influence on clouds (2). Atmospheric aerosols come from a combination of anthropogenic and natural sources and include both primary aerosols emitted directly to the atmosphere and secondary aerosols condensing from gaseous precursors. Aerosols above industrialized countries, such as the United States, until recently were generally assumed to be primarily of anthropogenic origin (e.g., ref. 3). Although climate models used in the fourth Intergovernmental Panel on Climate Change (IPCC) assessment include radiative forcing by a suite of anthropogenic aerosols, the radiatively significant aerosols are assumed to be sulfates from the oxidation of SO_2 (2) with estimated source of 92–126 TgS $year^{-1}$ (4).

Anthropogenic organics are generally estimated to provide a much smaller contribution to radiative forcing of the climate than sulfate aerosols (4). Anthropogenic primary organic aerosols are emitted by fossil fuel, biofuel, and agricultural burning. The IPCC climate models include black carbon emissions of 4.3–22 Tg $year^{-1}$ and organic carbon (OC) emissions of 17–77 Tg $year^{-1}$ (5). Current global aerosol models add a smaller contribution from secondary organic aerosols (SOA) of 12–70 TgC $year^{-1}$ formed from oxidation of gas phase precursors based on extrapolation of precursor emissions and laboratory-based SOA yields (6). Many recent observations have changed this view. There is now substantial evidence that the atmospheric SOA source is significantly larger than current models estimate (7, 8), and a much larger global SOA source of 140–910 TgC $year^{-1}$ has been proposed based on evaluation of the likely fate for VOCs emitted to the atmosphere, 90% of which are biogenic (9).

A large source of SOA should be observable with remote sensing techniques, particularly if it significantly impacts the atmospheric radiation budget. An aerosol source caused by BVOC oxidation should have a spatial pattern consistent with BVOC emissions, be highly seasonal with a maximum in summer, and follow the exponential dependence of BVOC emission with temperature. In this article, first we analyze the spatial and temporal distributions of column-integrated aerosol optical thickness (AOT) from satellite and ground-based remote sensing. Second, we provide evidence that the dominant seasonal signal in AOT over the SE U.S., and thus the summertime radiative forcing over this region, results from BVOC emissions reacting with anthropogenic pollution to form secondary aerosols. Third, we review available evidence for the spatial distribution of aerosol chemical components in the Eastern U.S., the relative importance of biogenic and anthropogenic contributions to the regional SOA in the SE U.S., and the interaction between biogenic and anthropogenic precursors in forming SOA. Finally, we estimate the radiative impacts of these aerosols for the region.

Observational Constraints

Remote sensing of AOT over dark land surfaces is possible from both satellite sensors and ground-based sunphotometers. These observations have been used to infer aerosol sources by exam-

Author contributions: A.H.G., C.D.K., C.L.H., and I.Y.F. designed research; A.H.G., C.D.K., and C.L.H. performed research; A.H.G., C.D.K., C.L.H., and I.Y.F. analyzed data; and A.H.G., C.D.K., C.L.H., and I.Y.F. wrote the paper.

The authors declare no conflict of interest.

[1]To whom correspondence may be addressed. E-mail: ahg@nature.berkeley.edu or ifung@berkeley.edu.

[2]Present address: Laboratoire des Sciences du Climat et l'Environnement, Gif-sur-Yvette, France.

[3]Present address: Department of Atmospheric Science, Colorado State University, Fort Collins, CO 80523.

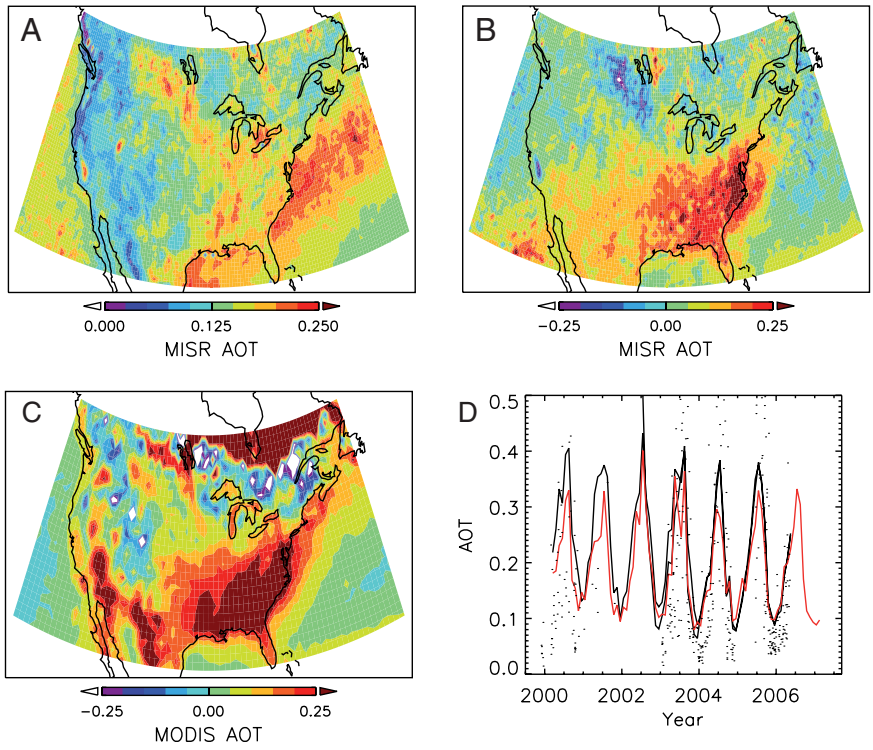

Fig. 1. Aerosol optical thickness (AOT) observed from 3 platforms. (*A*) MISR annual mean AOT map. (*B*) Map of difference between mean summer (JJA) and winter (DJF) AOT from MISR instrument. (*C*) same as *B* but for MODIS-TERRA instrument. (*D*) Time series of mean AOT over the SE U.S. from MISR (red line), MODIS-TERRA and MODIS-AQUA (black lines). Also shown are AERONET observations from the Walker Branch site (dots).

ining the spatial patterns of aerosol plumes (e.g., ref. 3). Because the residence time of aerosols is a few days to a week, they are concentrated near source regions. We therefore seek to identify characteristics of aerosol sources by examining the aerosol distributions in the atmosphere.

We use satellite remote sensing data from the MultiAngle Imaging Spectro-Radiometer (MISR; 10) and the Moderate Resolution Imaging Radiometer (MODIS; 11) to examine patterns in the AOT. MISR infers AOT by using observations with 9 cameras at different angles and separates scattering by the aerosol from scattering by the land surface based on the angular distribution of the up-welling radiance phase function (12). By contrast, MODIS infers AOT by comparing up-welling radiance at multiple wavelengths (13). MISR is aboard the National Aeronautics and Space Administration (NASA) Terra satellite, and MODIS is aboard the NASA Terra and Aqua satellites with AM and PM sun-locked polar orbits, respectively. Here, we use monthly mean 550-nm MISR and MODIS AOT observations from March 2000 to February 2007.

These satellite instruments have repeat intervals of 16 days with overlapping swath widths, resulting in MISR effectively imaging the planet approximately once per week and MODIS effectively imaging the planet approximately once every 2 days. Neither of these instruments can see aerosols if clouds are present, so coverage frequency varies with location and season. Although there can be some topographic bias error in absolute values of MISR AOT for a given season, this cancels out in the difference between seasons, which is the primary signal of interest here. Because these satellite-based instruments offer limited ability to observe higher-frequency variations, and we want to exclude the possibility that seasonal variations in surface reflectance lead to the observed patterns of aerosol variability, we also use data from the AERONET network of sunphotometers (14) to look at higher-frequency relationships such as the daily correlation between AOT and temperature. The AERONET instruments, like the satellites, use remotely sensed data that integrate over the entire atmospheric column; unlike the satellites, they are stationary and upward-looking and thus not strongly influenced by changes in surface reflectance. We use AERONET data with the Version 2 Inversion Algorithm (15). There are several possible sources of error in the AOT observations, including uncertainties in aerosol single-scattering albedo, mixing state, and size distribution (16), particularly considering questions of mixtures between anthropogenic and biogenic aerosols. Nonetheless, the agreement in the region of interest among the three different observations is good (17).

Spatial Patterns in Remote Sensing and Relationship with Temperature

Measurements by the MISR instrument reveal high AOT over the industrial Midwest and northeastern (NE) U.S. throughout the year, with an annual mean of 0.18 (Fig. 1*A*). Similarly high AOT (annual mean of 0.19) is observed over the SE U.S.. The AOT is higher in the summer than in the winter, and the seasonality (summer minus winter) is largest, ≈0.18, over the SE U.S. (Fig. 1*B*). The same spatial pattern of seasonality is observed by the MODIS instrument (Fig. 1*C*). The time series of AOT shows a clear, repeatable pattern of variations in the three instrument records: MISR and MODIS averaged over the SE region, and the ground-based AERONET station at Walker Branch, TN (Fig. 1*D*). We define the NE U.S. as 70–90°W and 37.5–45°N, and SE U.S. as 70–90°W and 30–37.5°N.

High-summertime AOT over the SE U.S. is not consistent with dominantly sulfate or anthropogenic carbon aerosols for several reasons. First, the geographic distribution of wet sulfate deposition (National Acid Deposition Program, available at http://nadp.sws.uiuc.edu) and sulfate concentration in aerosols (19) match the distribution of anthropogenic SO_2 emission, with maxima in the industrial Midwest and NE U.S. (Fig. 2*A*). Second, the observed AOT changes seasonally by a factor of 6–7 (summer(JJA)/winter(DJF), AERONET Walker Branch) whereas the sulfate changes seasonally by a smaller factor (≈3) as observed in the eastern U.S. by the Interagency Monitoring of Protected Visual Environments (IMPROVE) network. The IMPROVE sulfate seasonality is generally attributed to faster summertime oxidation of SO_2 through aqueous reactions with

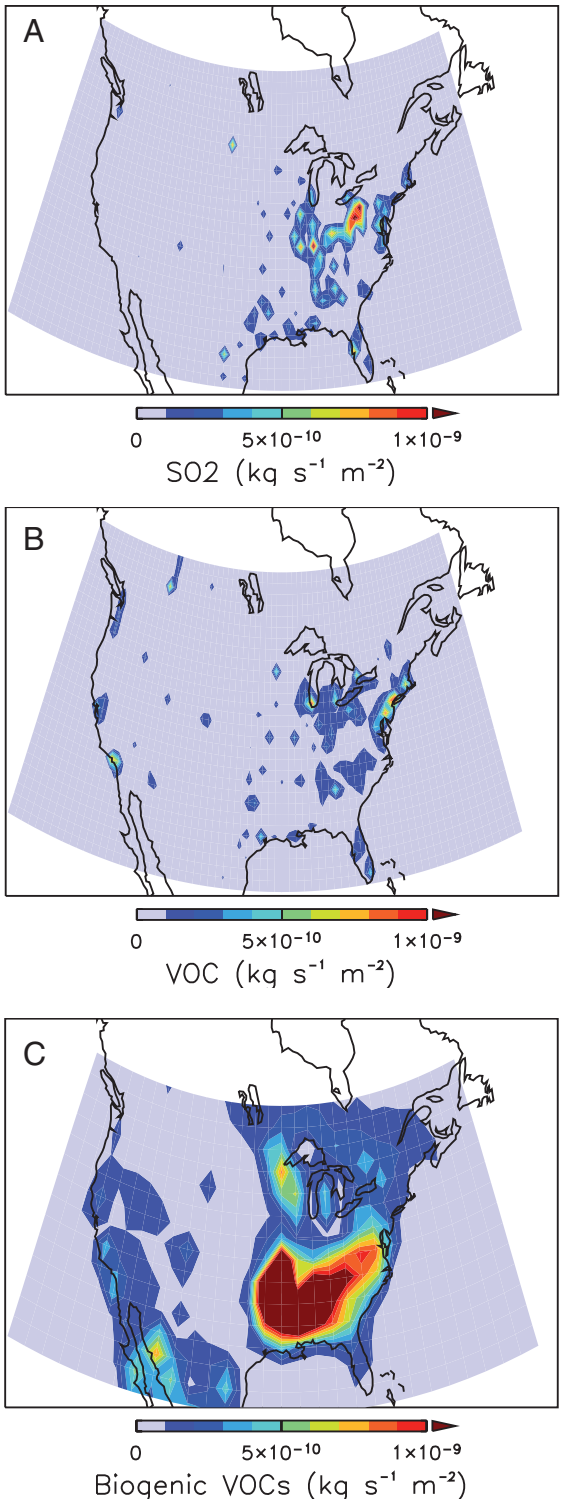

Fig. 2. Emission maps for the United States. (*A*) Annual total anthropogenic SO_2 emission. (*B*) Annual anthropogenic VOC emissions. (*C*) Annual total biogenic emissions of isoprene and monoterpenes. Anthropogenic Emissions are from U.S. Environmental Protection Agency National Emissions Inventory version 3 (NEI-99) (18), regridded from 4 km to 1° resolution.

peroxides (20). The main source of peroxides is isoprene oxidation in the SE U.S. (21), so we infer that the sulfate seasonality must be linked to BVOC emission and oxidation, but this seasonality is still insufficient to explain the observed AOT changes. Third, the observed pattern of AOT is also inconsistent

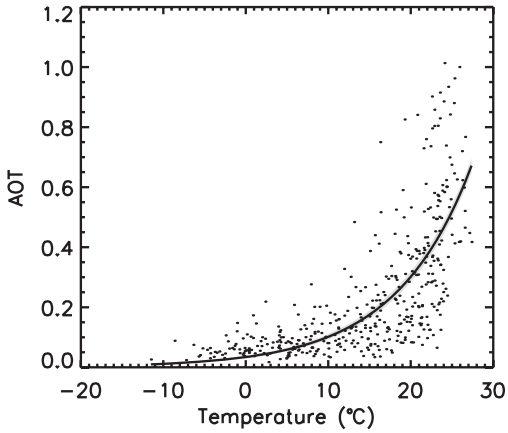

Fig. 3. Comparison of Walker Branch AERONET AOT (440 nm) vs. corresponding NCEP SE mean surface temperature reconstructions. Curve is exponential following the temperature dependence of biogenic VOC emission (28): $\gamma = \exp[\beta(T - T_S)]$, where β is an empirical coefficient of exponential dependence and T_S is the base temperature of standard conditions (303 K). The best-fit curve shown above ($R^2 = 0.55$) has a β of 0.11, in good agreement with BVOC emission observations.

with the spatial distribution of anthropogenic SOA precursor emissions, which are highest in the Northeast (Fig. 2*B*).

We hypothesize that the seasonal AOT pattern observed over the SE U.S. is driven by SOA from BVOC emissions. The seasonality of AOT and the spatial pattern of the AOT seasonal amplitude match those from BVOC emissions from forests in the SE U.S. (Fig. 2*C*). BVOC emissions for this region are primarily isoprene (81%) and monoterpenes (19%) and were calculated within the Community Land Model (CLM3) following Guenther et al. (22, 23) algorithms as described by Heald et al. (24). Current models of SOA production from isoprene and monoterpene oxidation based on laboratory chamber experiments use yields of 1–3% (25) and 2–23% (26), respectively. Current models do show that the large seasonal biogenic emission source in the SE U.S. leads to enhanced SOA over this region, qualitatively matching the spatial AOT signature we observe (27, 28); however, the SOA produced in these models is too small to dominate the total AOT signal, and therefore likely underestimates the magnitude of this source.

Formaldehyde and CO are both high-yield oxidation products of isoprene. Formaldehyde has been observed from the GOME and OMI instruments in space and used to confirm the large isoprene emission source in the SE U.S. (29, 30). Modeling of the spatial distribution of CO sources demonstrates that in summer BVOC oxidation is the dominant source of CO over the SE U.S. (31). These spatial and temporal patterns of observed formaldehyde, modeled CO from BVOC oxidation, and modeled isoprene emissions all match the AOT shown here, strengthening our argument for an observable link between BVOC oxidation and AOT.

To test our hypothesis further, we examined the relationship between the time series of AOT observed at the rural Walker Branch TN AERONET site and of surface temperature averaged over the SE region from NCEP reanalysis (32). Over all seasons, a high positive correlation ($R^2 = 0.55$) is found (Fig. 3), and the best-fit curve has an exponential temperature dependence ($\beta = 0.11$) in good agreement with the dependence of BVOC emissions (22). Although some of the correlation is because of their common seasonality, the correlation drops to ≈0.35 when lagged several days forward or backward, suggesting that at least 20% of the variance explained by this relationship is caused by short-term temperature-dependent processes such as VOC emission. In addition, separating the observations by season still reveals a significant temperature dependence during

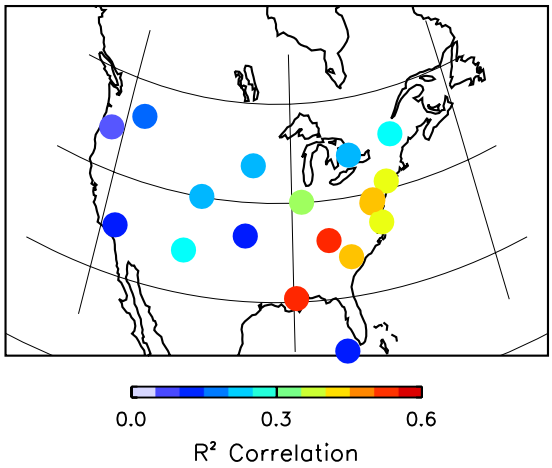

Fig. 4. R^2 correlation for the best-fit exponential curve of AOT vs. the corresponding NCEP mean temperature reconstruction, as in Fig. 3, for AERONET stations.

both the summer (JJA, $R^2 = 0.19$) and winter (DJF, $R^2 = 0.25$). We repeated this analysis for all other U.S. AERONET sites that had at least 2 years of data and found the strength of the temperature dependence of AOT throughout the eastern U.S. has a spatial dimension similar to the BVOC emissions (Fig. 4); this suggests that the biogenic signal can be observed throughout the eastern U.S. but that its relative importance to the total aerosol thickness decreases away from the rural SE U.S. peak BVOC source region.

We also compared the daily AERONET observations against NCEP relative humidity to test whether the observed seasonal variation in AOT could be caused solely by hygroscopic growth of aerosols. For the Walker Branch location, there is significant correlation between aerosol and humidity over all seasons, although the fraction of variance explained ($R^2 = 0.17$) is less than half that explained by the temperature relationship. When individual seasons are considered in isolation, there is not a significant relationship between humidity and aerosol in the summer ($R^2 = 0.01$) when the slope of the temperature–aerosol curve is steepest and thus temperature can play a strong role; whereas in the winter, when we expect temperature to be a relatively weak control, the aerosol–humidity correlation is highest ($R^2 = 0.24$). Thus, although there does seem to be a humidity component to the AOT observations, as expected, it cannot be driving the pattern we observe here.

Confirming that remotely sensed AOT is consistent with the mass expected from these precursors is currently difficult because of uncertainties in the size distribution, vertical profile, hygroscopic growth, and density of organic aerosols. However, the strong seasonal signal in AOT over the SE U.S. does suggest a larger SOA burden than previously simulated.

We hypothesized that the summertime maximum in AOT over the SE U.S. is dominated by S arising from biogenic VOC oxidation in the presence of anthropogenic pollutants. The spatial pattern of aerosol seasonality supports this hypothesis, as does the functional relationship between daily aerosol and temperature.

Evidence of Aerosol Chemical Composition in the Eastern U.S.

Multiple studies have reported findings consistent with our hypothesis but have not advanced the hypothesis themselves. Organics contribute a substantial fraction of aerosols observed downwind of the densely populated and highly industrialized eastern U.S. (33) and over much broader regions including urban, rural, and remote environments, as shown by aerosol mass spectrometer (AMS) measurements (34). The average spatial distributions of sulfate, nitrate, and carbon in aerosol in the eastern U.S. differ significantly. The maximum carbon occurs in the SE U.S. (e.g., Georgia), whereas the maxima sulfate and nitrate occur much further north (e.g., Ohio) based on rural IMPROVE network and urban Speciation Trends Network (STN) surface observations (19). The organic aerosol in the SE U.S. is mostly secondary, with radiocarbon (^{14}C) measurements indicating 70% or more of the carbon is modern (rather than fossil) in rural locations and therefore likely of biogenic origin (35, 36).

Further evidence for the presence of BVOC oxidation products in SOA in this region is provided by site-specific analysis of the organic chemical composition of PM2.5 (37, 38). At Research Triangle Park, NC, in summer 2003, ambient PM2.5 consisted on average of 41% organic matter, 2% elemental carbon, 12% ammonium, and 37% sulfate, with higher organic and PM2.5 concentrations under acidic conditions. An organic tracer-based method was used to estimate the contributions of SOA from biogenic isoprene and terpenes, anthropogenic precursors, and biomass burning to total OC. The relative contributions were found to be highly seasonal, with SOA from biomass burning accounting for >50% of OC in winter when SOA contributions were low, and contributions from BVOC accounting for >50% of OC in July and August, with twice as much total OC in July–August compared with January–February.

Forty distinct polar organic species originating from terpene oxidation were identified, comprising 7.2% on average of the total in fine aerosol organic mass, on filters collected in the SE U.S. in June 2004, at three sites in the Southeastern Aerosol Research and Characterization (SEARCH) network (Jefferson Street, Atlanta, GA; Birmingham, AL; Centreville, AL) (39). Measurements of ^{14}C in secondary organic aerosol over a full annual cycle at the same sites demonstrate that fossil C contributions are higher at urban sites and do not change much seasonally, whereas the modern C contribution is similar at all sites with much higher concentrations in spring and summer, consistent with a dominant summertime contribution from BVOC oxidation distributed over a broad region (40). In summer, isoprene-derived SOA correlated positively with the modern SOA, demonstrating a large contribution to total SOA in summer.

In contrast, surface-based filter measurements from the IMPROVE network indicate low fractions of organic aerosol in the SE U.S. However, MISR, MODIS, and AERONET all detect substantially more aerosol in the atmospheric column over the SE relative to the NE U.S. in summer than the IMPROVE network detects at the ground (41). We infer from this discrepancy that much of the organic secondary addition to the aerosol in the southeast must occur above the surface layer. This is consistent with in situ aircraft data (42–44), where the organic fraction of the total aerosol has been shown to increase with height, even though surface sulfate concentrations were much larger than surface organic concentrations. Similarly, Kleinman et al. (45) show that aloft outside of urban regions throughout the eastern U.S., the organic fraction dominates the total aerosol mass with average concentrations of 6.5 and 11 $\mu g\ m^{-3}$, respectively. Consistent with photochemical production after convective transport of BVOC precursors are vertical profile observations of peroxides in this region, with maxima between 1 and 4 km (21). It therefore seems likely that the increase in organic/sulfate ratio with altitude results at least partially from heterogeneous chemical reactions adding BVOC oxidation products to the preexisting aerosol and is also consistent with gas phase semivolatile VOC oxidation products partitioning onto aerosol with cooler temperatures aloft. Modeling studies of SOA production from isoprene oxidation over the U.S. predict a strong vertical profile with ≈10% of SOA simulated to occur in the surface layer (0–35 m), ≈80% occurring in the planetary boundary layer (0–2.85 km), and ≈10% occurring in the free troposphere (2.85–9 km) (46), whereas the maximum contribu-

tion from terpene oxidation to SOA maximizes at lower altitudes (24). New observations of aerosol chemical and optical properties as a function of altitude in the summer and winter will be required to confirm definitely the source of this seasonally high AOT over the SE US.

Evidence for Chemical Interactions Between Biogenic and Anthropogenic Precursors Forming SOA

Recent evidence suggests that there are chemical interactions between anthropogenic and biogenic aerosol precursors that are important in the formation of secondary aerosols in the SE U.S. Gao et al. (39) used chemical and correlation analyses to suggest that the polar organics they detected originated from terpene oxidation in the presence of anthropogenic NO_x and SO_2 and that the three inland SE U.S. SEARCH sites in Georgia and Alabama had a consistent distribution of chemical composition, whereas the terpene oxidation products were not found to be as prominent at a coastal site in Pensacola, FL, where the prevailing wind is from the Gulf of Mexico, concluding that a biogenic SOA source is likely ubiquitous in this continental region. Following on this work, Surratt et al. (47–49) proposed a mechanism for organosulfate formation from isoprene and terpene oxidation based on experiments with both OH (daytime) and NO_3 (nighttime) as oxidants. In laboratory experiments, the rate of SOA formation increased with the concentration of sulfuric acid seed aerosols, and the chemical nature of SOA formed from terpenoid compound oxidation depends strongly on NO_x concentrations. Furthermore, they observed the same and similar compounds in ambient aerosols in the SE U.S. and quantified that organosulfates account for up to 30% of the organic aerosol mass in K-puszta, Hungary. Similar to these observations, secondary aerosol growth in pollution plumes enhanced in both SO_2 and VOC downwind of Houston, TX, was observed to exceed greatly that expected from SO_2 or VOC alone, suggesting that the presence of SO_2 was key to the growth of secondary organic aerosols (50). The compounds identified and the radiocarbon data for this region, and the mechanisms proposed by Surratt et al. provide a potentially critical link between many recent observations, such as that aerosol in the eastern U.S. have a large organic component (42), that heterogeneous atmospheric aerosol production can occur by acid-catalyzed particle phase reactions (51), that the transformation of BVOC to SOA may be mediated by the presence of anthropogenic pollution based on correlations between SOA and anthropogenic pollutants (36), and the spatial and temperature-dependent observations of AOT presented here. These findings together point to a large source of SOA from BVOC oxidation, especially in the presence of pollution.

Radiative Impacts

The most recent IPCC assessment estimates that all aerosols contribute a direct radiative effect of -5.4 ± 0.9 W m^{-2} in the global mean and that anthropogenic sulfate contributes a global annual mean negative radiative forcing of -0.4 W m^{-2}, which can be compared with the positive forcing from greenhouse gas emissions ($+2.6$ W m^{-2}). We estimate top of the atmosphere (TOA) radiative change (ΔF) for optically thin atmosphere as (52):

$$\Delta F = -DS_0T_{atm}^2(1-A_c)\bar{\omega}\beta AOT\left((1-R_s)-\frac{2R_s}{\beta}\left(\frac{1}{\bar{\omega}}-1\right)\right) \quad [1]$$

where D, fractional day length = 1/2; S_o, solar constant = 1,370 W/m^2; T_{atm}, atmospheric transmission = 0.76; A_c, fractional cloud amount = 0.6; $\bar{\omega}$, single scattering albedo = 0.972 (53); β, up-scatter fraction = 0.21; R_s, surface reflectance = 0.15. All other values were taken from ref. 52. The seasonal change in AOT (0.18, based on the MISR AOT summer minus winter difference) observed over the SE U.S. implies a regional direct clear-sky radiative effect of -3.9 W m^{-2} in summer, comparable with the regional sulfate radiative forcing in the NE U.S.

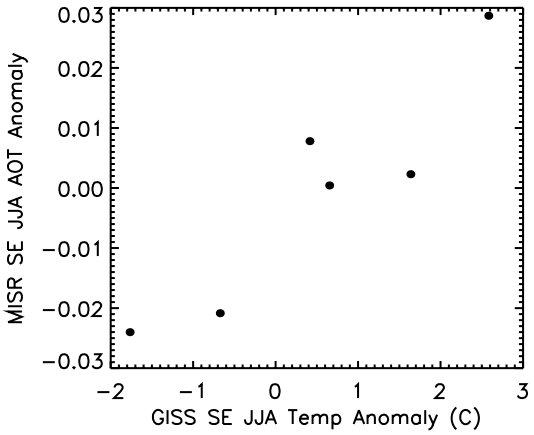

Fig. 5. Interannual anomalies in summertime southeast regional mean temperature vs. aerosol optical thickness, for years 2000–2005. Temperature is from Goddard Institute for Space Studies Surface Temperature (GISTEMP) analysis (55), AOT is from MISR.

The -3.9 W m^{-2} greater radiative cooling in summer cannot be treated strictly as radiative forcing, i.e., an anthropogenic forcing, because the aerosols are mainly from the oxidation of BVOC emitted from forests. However, as shown above, the AOT includes aerosol contributions resulting from the interaction between natural BVOC emissions and anthropogenic pollution and therefore an additional radiative forcing that may be modulated by anthropogenic activities and that has not been considered. If there are systematic seasonal variations, e.g., in surface albedo, cloud cover, or aerosol microphysical properties, these could cause uncertainty in our radiative effect calculation. It is premature to compare our estimate directly with IPCC estimates of radiative forcing by aerosols because the regional and temporal extents of the AOT from BVOC–pollution interactions remain to be established. We note that the current generation of models underestimates the seasonality of aerosols in this region (54) and thus may be overestimating radiative forcing by direct anthropogenic aerosol source relative to a biogenic or combined source.

The observed seasonal temperature dependence of the AOT is also reflected in interannual covariation between mean summertime regional temperature and aerosol (Fig. 5). Although there are relatively few years of satellite aerosol measurement to establish a strong relationship, the observations spanning the period 2000–2005 are consistent with the idea that warm summers lead to higher BVOC emission. This relationship could also possibly be related to more power consumption for air conditioners causing increased NO_x emissions, or to annually varying transport patterns, but there is clearly a relationship of AOT varying interannually with temperature. Thus, we predict higher regional summertime aerosol levels in the future and a regional negative, albeit small, feedback on warming and a less rapid increase in BVOC emissions and AOT.

Conclusions

AOT over the SE U.S. has a strong seasonal cycle of 0.18 corresponding to a stronger radiative impact (-3.9 W m^{-2} cooling) in summer than in winter. The spatial pattern of this AOT seasonality matches BVOC emissions and does not match the dominant spatial patterns of anthropogenic emissions. Temporal variations in AOT in the region also follow a functional relationship with temperature that matches BVOC emissions dependence on a daily time scale. Together, these patterns

suggest that BVOC emissions oxidizing to form SOA, likely modulated by anthropogenic emissions, are responsible for a large fraction of the total column aerosol load in the region. The recently reported mechanism of organosulfate formation from heterogeneous oxidation of BVOC in the presence of NO_x and acidic seed aerosols provides another likely link between these observations, with an additional pathway for the formation of these secondary aerosols.

Seasonal and interannual variations of aerosol over the region demonstrate that in the presence of current anthropogenic emissions, the temperature dependence of BVOC emission leads to SOA increasing rapidly with temperature, thus SOA appears to act as a negative climate feedback regionally.

Radiative forcing as the term is used by the IPCC is anthropogenic in origin. Because biogenic SOA is generally defined as natural aerosol, climate and aerosol models assessing radiative forcing neglect this biogenic SOA. Multiple studies discussed here are consistent with our interpretation that anthropogenic emissions exert control over the amount of biogenic SOA produced, and therefore it may be necessary to include organic aerosol forcing as a radiative forcing in climate models. Assuming that the Earth's climate warms in the future as projected by IPCC (2), BVOC emissions will also increase as will SOA unless the anthropogenic emissions are decreased.

If BVOC emissions are truly transformed to SOA dominantly through reactions with regional anthropogenic emissions as suggested, efforts to reduce aerosol in this region must focus on controlling anthropogenic NO_x, SO_2, and primary OC emissions, similar to the regulatory measures that regional ozone and acid deposition problems have required in the past. Managing regional haze and visibility in the SE U.S. and modeling air quality interactions with future climate will require improved quantitative understanding of the photochemical processes controlling BVOC and anthropogenic emissions reacting to form SOA.

ACKNOWLEDGMENTS. We thank the AERONET, MISR, and MODIS teams for use of their data. C. D. K. was supported by a National Aeronautics and Space Administration Earth System Science Fellowship NNG04GQ76H, and C. L. H. was supported by a National Oceanic and Atmospheric Administration Climate and Global Change Postdoctoral Fellowship.

1. Chameides W, Lindsay R, Richardson J, Kiang C (1988) The role of biogenic hydrocarbons in urban photochemical smog: Atlanta as a case study. *Science* 241:1473–1475.
2. IPCC (2007), *Climate Change 2007*: *The Physical Science Basis*, Solomon S, et al., eds (Cambridge Univ Press, Cambridge, UK).
3. Kaufman YJ, Tanre D, Boucher O (2002) A satellite view of aerosols in the climate system. *Nature* 419:215–223.
4. Haywood J, Boucher O (2000) Estimates of the direct and indirect radiative forcing due to tropospheric aerosols: A review. *Rev Geophys* 38:513–543.
5. Bond TC, et al. (2004) A technology-based global inventory of black and organic carbon emissions from combustion. *J Geophys Res* 109:D14203.
6. Kanakidou M, et al. (2005) Organic aerosol and global climate modelling: A review. *Atm Chem Phys* 5:1053–1123.
7. Heald C, et al. (2006) Trans-Pacific transport of Asian anthropogenic aerosols and its impact on surface air quality in the United States. *J Geophys Res* 111:D14310.
8. Volkamer R, et al. (2006) Secondary organic aerosol formation from anthropogenic air pollution: Rapid and higher than expected. *Geophys Res Lett* 33:L17811.
9. Goldstein AH, Galbally IE (2007) Known and unexplored organic constituents in the Earth's atmosphere. *Env Sci Tech* 40:1514–1521.
10. Kahn R, et al. (2005) MultiAngle Imaging Spectroradiometer (MISR) global aerosol optical depth validation based on 2 years of coincident Aerosol Robotic Network (AERONET) observations. *J Geophys Res* 110:D10S04.
11. Kaufman YJ, et al. (1997) Operational remote sensing of tropospheric aerosol over land from EOS Moderate Resolution Imaging Spectroradiometer. *J Geophys Res* 10:17051.
12. Martonchik JV, et al. (1998) Techniques for the retrieval of aerosol properties over land and ocean using multiangle imaging. *IEEE Trans Geosci Rem Sens* 36:1212–1227.
13. King MD, Kaufman YJ, Tanre D, Nakajima T (1999) Remote sensing of tropospheric aerosols from space: Past, present, and future. *Bull Am Met Soc* 80:2229–2259.
14. Holben BN, et al. (1998) AERONET: A federated instrument network and data archive for aerosol characterization. *Rem Sens Env* 66:1–16.
15. Dubovik O, King MD (2000) A flexible inversion algorithm for retrieval of aerosol optical properties from sun and sky radiance measurements. *J Geophys Res* 105:20673.
16. Wang J, Martin ST (2007) Satellite characterization of urban aerosols: Importance of including hygroscopicity and mixing state in the retrieval algorithms. *J Geophys Res* 112:D17203.
17. Abdou W, et al. (2005) Comparison of coincident MultiAngle Imaging Spectroradiometer and Moderate Resolution Imaging Spectroradiometer aerosol optical depths over land and ocean scenes containing aerosol robotic network sites. *J Geophys Res* 110:D10S07.
18. US Environmental Protection Agency (2004) EPA clearinghouse for inventories and emissions factors: 1999 national emission inventory documentation and data. Final version 3.0 (Tech Rep 2004; available at www.epa.gov/ttn/chief/net/1999inventory.html).
19. Rao V, Frank NF, Rush AR, Dimmick F (2003) Chemical speciation of PM2.5 in urban and rural areas. National Air Quality and Emissions Trends Report, 2003 Special Studies (US Environmental Protection Agency, Washington, DC).
20. Chin M, et al. (2000) Atmospheric sulfur cycle simulated in the global model GOCART: Comparison with field observations and regional budgets. *J Geophys Res* 105(D20):24689–24712.
21. Snow J, et al. (2007) Hydrogen peroxide, methyl hydroperoxide, and formaldehyde over North America and the North Atlantic. *J Geophys Res* 112:D12S07.
22. Guenther A, et al. (1995) A global model of natural volatile organic compound emissions. *J Geophys Res* 100:8873–8892.
23. Guenther A, et al. (2006) Estimates of global terrestrial isoprene emissions using MEGAN (Model of Emissions of Gases and Aerosols from Nature). *Atm Chem Phys* 6:3181.
24. Heald CL, et al. (2008) Predicted change in global secondary organic aerosol concentrations in response to future climate, emissions, and land-use change. *J Geophys Res* 113:D05211.
25. Kroll JH, Ng NL, Murphy SM, Flagan RC, Seinfeld JH (2005) Secondary organic aerosol formation from isoprene photooxidation under high-NO_x conditions. *Geophys Res Lett* 32:L18808.
26. Griffin RJ, Cocker DR, Seinfeld JH, Dabdub D (1999) Estimate of global atmospheric organic aerosol from oxidation of biogenic hydrocarbons. *Geophys Res Lett* 26:2721.
27. Chung S, Seinfeld JH (2002) Global distribution and climate forcing of carbonaceous aerosols. *J Geophys Res* 107(D19):4407.
28. Henze DK, Seinfeld JH (2006) Global secondary organic aerosol from isoprene oxidation. *Geophys Res Lett* 33:L09812.
29. Palmer P, et al. (2003) Mapping isoprene emissions over North America using formaldehyde column observations from space. *J Geophys Res* 108:4180.
30. Millet DB, et al. (2007) Spatial distribution of isoprene emissions from North America derived from formaldehyde column measurements by the OMI satellite sensor. *J Geophys Res* 113:D02307.
31. Hudman RC, et al. (2008) Biogenic versus anthropogenic sources of CO in the United States. *Geophys Res Lett* 35:L04801.
32. Kalnay E, et al. (1996) The NCEP/NCAR 40-year reanalysis project. *Bull Am Meteorol Soc* 77:437.
33. Novakov T, Hegg D, Hobbs P (1997) Airborne measurements of carbonaceous aerosols on the East Coast of the United States. *J Geophys Res* 102(D25):30023–30030.
34. Zhang Q, et al. (2007) Ubiquity and dominance of oxygenated species in organic aerosols in anthropogenically-influenced northern hemisphere midlatitudes. *Geophys Res Lett* 34:L13801.
35. Bench G, Fallon S, Schichtel B, Malm W, McDade C (2007) Relative contributions of fossil and contemporary carbon sources to PM2.5 aerosols at nine interagency monitoring for protection of visual environments (IMPROVE) network sites. *J Geophys Res* 112:D10205.
36. Weber RJ, et al. (2007) A study of secondary organic aerosol formation in the anthropogenic-influenced southeastern United States. *J Geophys Res* 112:D13302.
37. Kleindienst TE (2007) Estimates of the contributions of biogenic and anthropogenic hydrocarbons to secondary organic aerosol at a southeastern US location. *Atm Env* 41:8288–8300.
38. Lewandowski M, Jaoui M, Kleindienst TE, Offenberg JH, Edney EO (2007) Composition of PM2.5 during the summer of 2003 in Research Triangle Park, North Carolina. *Atm Env* 41:4073–4083.
39. Gao S, et al. (2006) Characterization of polar organic components in fine aerosols in the southeastern United States: Identity, origin, and evolution. *J Geophys Res* 111:D14314.
40. Ding X, Zheng M, Edgerton ES, Jansen JJ, Wang X (2008) Contemporary or fossil origin: Split of estimated secondary organic carbon in the Southeastern United States. *Environ Sci Technol* 42:9122–9128.
41. Malm WC, Schichtel BA, Pitchford ML, Ashbaugh LL, Eldred RA (2004) Spatial and monthly trends in speciated fine particle concentration in the United States. *J Geophys Res* 109:D03306.
42. Novakov T, Hegg D, Hobbs P (1997) Airborne measurements of carbonaceous aerosols on the East Coast of the United States. *J Geophys Res* 102(D25):30023–30030.
43. Hegg D, Livingston J, Hobbs P, Novakov T, Russell P (1997) Chemical apportionment of aerosol column optical depth off the Mid-Atlantic coast of the United States. *J Geophys Res* 102(D21):25293–25303.
44. Heald C, et al. (2005) A large organic aerosol source in the free troposphere missing from current models. *Geophys Res Lett* 32:L18809.
45. Kleinman L, et al. (2007) Aircraft observations of aerosol composition and ageing in New England and Mid-Atlantic States during the summer 2002 New England Air Quality Study field campaign. *J Geophys Res* 112:D09310.
46. Zhang Y, Huang JP, Henze DK, Seinfeld JH (2007) Role of isoprene in secondary organic aerosol formation on a regional scale. *J Geophys Res* 112:D20207.
47. Surratt JD, et al. (2007) Effect of acidity on secondary organic aerosol from isoprene. *Env Sci Tech* 41:517.
48. Surratt JD, et al. (2008) Organosulfate formation in biogenic secondary organic aerosol. *J Phys Chem A* 112:8345–8378.
49. Surratt JD, et al. (2006) Chemical composition of secondary organic aerosol formed from the photooxidation of isoprene. *J Phys Chem A* 110:9665–9690.
50. Brock C, et al. (2003) Particle growth in urban and industrial plumes in Texas. *J Geophys Res* 108(D3):4111.
51. Jang M, Czoschke N, Lee S, Kamens R (2002) Heterogeneous atmospheric aerosol production by acid-catalyzed particle-phase reactions. *Science* 298:814–817.
52. Haywood JM, Shine KP (1995) The effect of anthropogenic sulfate and soot aerosol on the clear sky planetary radiation budget. *Geophys Res Lett* 22:603.
53. Köpke P, Hess M, Schult I, Shettle EP (1997) Global Aerosol Dataset, Tech Rep 243 (Max-Planck Inst Meteorol, Hamburg, Germany).
54. Kinne S, et al. (2006) An aerocom initial assessment: Optical properties in aerosol component modules of global models. *Atm Chem Phys* 6:1815–1834.
55. Hansen J, Ruedy R, Glascoe J, Sato M (1999) GISS analysis of surface temperature change. *J Geophys Res* 104(D24):30997–31022.